DNS AND ENGINEERING MODELING OF THE ELECTROSLAG REMELTING PROCESS

Jérémy Chaulet[1,3], Abdellah Kharicha[2], Bernard Dussoubs[1], Sylvain Charmond[3], Alain Jardy[1], Stéphane Hans[3]

[1]Institut Jean Lamour (UMR 7198 Université de Lorraine / CNRS), Campus Artem - BP 50840, F-54011 NANCY Cedex, LabEx DAMAS, France
[2]Christian Doppler Laboratory for Metallurgical Applications of MHD, A-8700 LEOBEN, Austria
[3]Aubert & Duval (ERAMET Group), BP 1, F-63770 LES ANCIZES, France

Keywords: ElectroSlag Remelting (ESR), slag hydrodynamics, metal droplets, multiphase modeling

Abstract

Electroslag remelting (ESR) is a process extensively used to produce metallic ingots with high quality standards. In order to investigate the possibly important impact of the behavior of liquid metal droplets in the slag on the solidification of the ingot, 3D VOF and engineering modeling have been associated. At MU Leoben, several 3D simulations were performed to explore the effects of the electric current and electrode immersion depth on the dripping phenomena. Simultaneously a 2D multiphase model was used to estimate the distribution, speed, and overheat of the droplets entering the liquid pool. With adequate adaptations, the results given by this computationally cheap 2D model can fit the 3D results. The aforementioned results will be used to improve a 2D engineering model previously developed at IJL Nancy, aimed to help optimizing the operating parameters. To improve process knowledge, several remelting experiments at industrial scale were performed under various geometrical and electrical conditions.

Introduction

Electroslag remelting (ESR) is a leading process to produce alloys for critical applications – such as tooling, energy or aeronautics – which require high metallurgical quality. The slag is at the heart of this remelting process: chemical and electrochemical reactions with the melted alloy enable metal refining and, above all, the thermal energy needed to melt the electrode is supplied by Joule heating since an electric current goes through this highly resistive medium [1]. Liquid metal droplets hence form on the immersed tip of the electrode and fall through the liquid slag. Both molten slag and liquid metal flows are largely driven by electromagnetic forces.

Liquid metal droplets are the first energy carriers to the liquid pool. For example, according to Ballantyne [2], only a few percent of the heat received by the ingot is supplied by conduction at the interface. Following modeling works offer similar heat balances [3, 4]. Thereby, we can assume that the way these liquid droplets enter the liquid pool, i.e. their repartition and their overheat, can influence the momentum and enthalpy distribution within the melt pool. Consequently, the final ingot quality might be impacted.

In most of ESR 2D models, droplets formation and their behavior while passing through the slag are simplified or neglected. A simple way to consider the impact of droplets on the ingot is to model a homogeneous liquid metal flux at the slag/pool interface [5]. Droplets overheat can also be extracted from the slag cylinder below the electrode and spread in the whole melt pool [3]. A user defined velocity profile can be used to reflect a non-homogeneous distribution of droplets [6]. Karimi-Sibaki et al. modeled this influence on mass, momentum and energy by using a defined impact depth of the droplets [7].

In all these methods, the distribution of energy and momentum carried by the droplets either is an assumption of the model or explicitly defined by the user. Therefore, these models are not able to describe a variation in the droplets impact resulting from a variation in the operating conditions. The only attempt known by the authors was made by Giesselmann et al. [8]. A 3D model is used to simulate the dripping phenomena at small time-scale. A time-averaged flow is then transferred to a model that simulates the slag and liquid pool behavior and the ingot solidification. Even with a weak coupling scheme, this model combination may remain computationally expensive.

Thanks to recent 3D simulations [9], the dripping phenomena in ESR is better understood, and new approaches to model droplets behavior in 2D models can be conceived. In this paper, the development of a 2D multiphase model is described, which aims to predict the droplets distribution and overheat for a lower computational cost. Such a calculation will eventually be implemented within an engineering model to predict the droplets behavior under varying operating conditions and their impact on the final ingot. A summary of our approach is given in Figure 1.

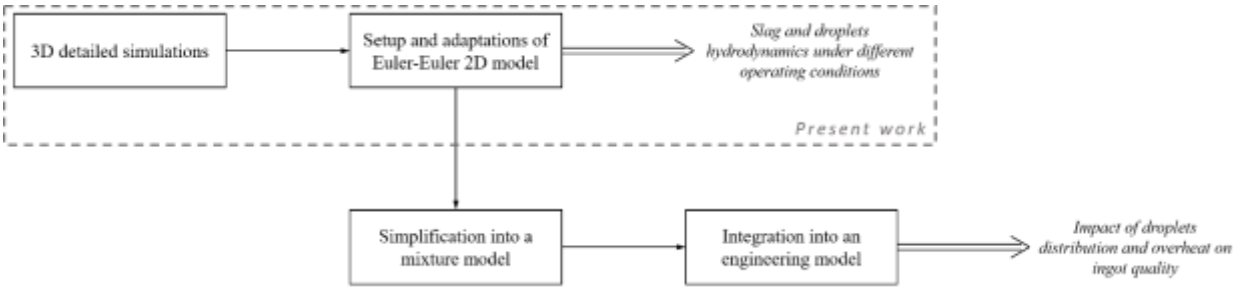

Fig. 1: Droplets behavior modeling route from 3D detailed simulation to engineering modeling

This research project is the fruit of a collaboration between two academic partners – the Metallurgical Process Engineering group of Institut Jean Lamour (Nancy, France) and CD Laboratory for Metallurgical Applications of MHD (Leoben, Austria) – and an industrial company – Aubert & Duval (Les Ancizes, France). This new collaboration makes it possible to cover a wide modeling approach, and to support these developments thanks to specifically designed trial ingots.

Modeling Approaches

As discussed above, the modeling tasks of this project rely on the previous works of the two academic groups to develop a new approach to study the impact of metal droplets behavior in electroslag remelting. In this section, pre-existing and recently developed models are successively presented.

3D Simulations

As described in previous works [9], 3D simulations of the dripping phenomena and the slag hydrodynamics can be performed using the CFD software ANSYS Fluent. Here, the fully coupled electromagnetic field is calculated in 3D, thanks to a self-developed MHD module. The fluid calculation domain is divided into 11.9 million volume elements. The computational domain includes a layer of slag and a layer of liquid steel. The geometrical reconstruction VOF approach is used for the interface tracking. The mesh is refined at vicinity of all wall boundaries, especially near the electrode where a thin liquid film (~1 mm) develops during the melting. Thanks to the very large number of volume element, effects of the turbulence can be estimated with the standard Smagorinsky large eddy simulation (LES) model.

The interface between the air and the slag, known as the exposed slag surface, is modelled with a slipping fixed wall. During the process the solid electrode can develop a flat or a parabolic surface, here it is assumed flat. Different electrode immersion depths can be assumed. However the process of electrode melting is not predicted but imposed, the electrode is assumed to melt uniformly over its tip surface.

The electromagnetic field is calculated, in a fully coupled way, thanks to a self-developed magnetohydrodynamic module. In the latest, a potential formulation is used for the electric and the magnetic field. The Lorentz forces and the Joule heating are recalculated at each time step, according to the electromagnetic field which in turn depends on the phase distribution. A sinusoidal electric current is applied between the electrode and the bottom boundary. The occurrence of eddy current is naturally predicted for each time step. Due to inertia effect, the mean flow is not sensitive to the too fast variation of the 50Hz electric current. However this is not true for the dripping phenomena, the time scale associated with droplet dynamics (departure and falls) was found too close to the time scale associated with the electric current (50Hz). This results in strong effects of the eddy currents on the liquid metal faucets and droplets.

Engineering Model

A 2D axisymmetric model of the ESR process, named SOLECS (which stands for SOLar-type-Esr-Complete-Simulation), has been developed at Institut Jean Lamour since 2004. It has been successfully compared with trial remeltings for validation, and is now routinely used at Aubert & Duval facility.

Details about this engineering model and its construction may be found in previous papers [10, 11]. Briefly, SOLECS simulates the continuous growth of the ESR ingot and its subsequent cooling. Coupled heat and momentum transfers are solved in both slag and ingot using a finite volume approach. Solidification is addressed via a continuum mixture method. Turbulence is estimated thanks to a RANS k-ε model. The slag-liquid pool interface is assumed to be flat, and the immersion depth of the electrode is constant during the entire simulation, with a non-deformable electrode/slag interface. Liquid metal droplets are not explicitly represented, as this model is monophasic by nature.

The electromagnetic field is computed based on the reduction of Maxwell's equations into a single one. Its computational domain covers the electrode, slag, ingot and mold, in order to be able to calculate the amount of current crossing the solidified slag.

Finally, the calculation of local solidification conditions, such as the local solidification time (LST) or solidification front angle, make this model suitable for the evaluation – with adequate criteria – of the final ingot quality.

2D Diphasic Model of the Slag and Drops

Based on an Euler-Euler approach, the two phases considered are modeled as an interpenetrating continuum. The continuous phase is the liquid slag and the disperse phase is constituted by liquid metal drops. The CFD software ANSYS Fluent is used to solve the coupled transfers of momentum and enthalpy, based on the resolution of the Navier-Stokes equations for each phase, in their Reynold-Averaged approximation. Considering momentum exchange, the drag force is calculated using Schiller-Naumann correlations to determine the drag coefficient [12]. A standard k-ε model is applied to estimate the intensity of turbulence in each phase.

Heat transfer is also solved for each phase, and both slag and metal are considered only in the liquid state. A Ranz-Marshall formula is used to estimate the interphase heat transfer coefficient [13].

As in the case of SOLECS, an electromagnetic model has been developed to calculate the fully coupled magnetic induction field. The equation for the magnetic field, derived from Maxwell's equations, is given by Eq. 1 for a 2D computation in cylindrical coordinates. μ_0 is the magnetic permeability, and σ denotes the electrical conductivity.

$$\frac{\partial B_\theta}{\partial t} + \frac{\partial}{\partial z}\left(\frac{1}{\sigma\mu_0}\frac{\partial B_\theta}{\partial z}\right) + \frac{\partial}{\partial r}\left(\frac{1}{\sigma\mu_0}\frac{1}{r}\frac{\partial (rB_\theta)}{\partial r}\right) = 0 \tag{1}$$

The phasor representation is used to compute the field induced by an alternating current. A phasor, also called complex amplitude, is a complex number used to represent a sinusoidal function of time.

Time-averaged Lorentz forces are then calculated using Eq. 2, and are added as a source term to the momentum transfer equations. The power dissipated by Joule heating is also computed (Eq. 3) and added as a source term to the heat transport equations. In Eq. 2 and 3, $\vec{J}$ is the current density vector field, $\sim$ indicates the phasor representation and * stands for the conjugate complex number.

$$\vec{F}_{Lo} = Re\left(1/2\,\tilde{\vec{J}} \times \widetilde{B_\theta}^{\,*}\right) \tag{2}$$

$$Q_{Joule} = Re\left(1/2\sigma\,\tilde{\vec{J}} \times \tilde{\vec{J}}^{\,*}\right) \tag{3}$$

The computational domain is schematically shown in Figure 2. It covers the whole slag bath and contains also the lower part of the electrode and the upper part of the ingot. Physical properties needed as input data for this model, along with typical values used, are presented in Table 1.

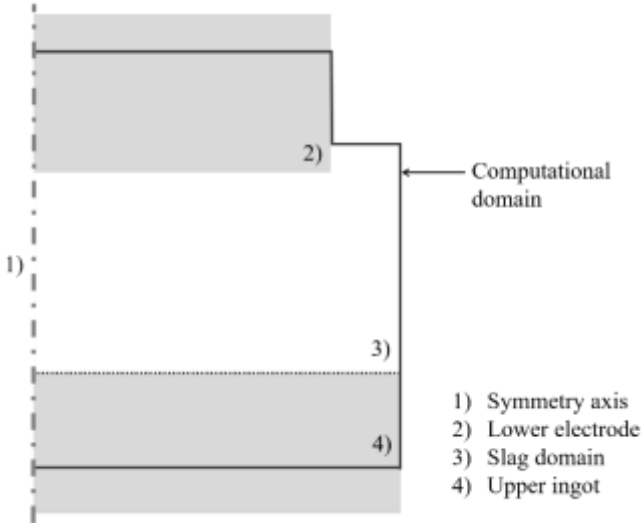

Fig. 2: Schematic representation of the computational domain

	Liquid metal (low-alloyed steel)	Slag (70/15/15 type)
Dynamic viscosity η ($kg.m^{-1}.s^{-1}$)	0.006	0.008
Density ρ ($kg.m^{-3}$)	6940	2765
Thermal expansion coefficient β (K^{-1})	$1.1\ 10^{-4}$	$7.5\ 10^{-5}$
Thermal conductivity λ ($W.m^{-1}.K^{-1}$)	30	35
Specific heat capacity C_p ($J.kg^{-1}.K^{-1}$)	690	1380
Electrical conductivity σ ($\Omega^{-1}.m^{-1}$)	10^6	250

Table 1: Thermo-physical properties of liquid metal and slag used in the simulations

Some Recent Enhancements of the 2D Diphasic Model

The precise dripping phenomena cannot be accurately modeled with such a uniform Euler-Euler approach, as the liquid metal behavior is not identical in the whole resolution domain. The 3D simulation helps us to underline the major effects that need to be accounted for in a lower order model.

Electrical Conductivity Averaging

As in all volume-averaged methods, the estimation of cell-averaged properties is of great importance. The averaging formula used can strongly influence the computed flow behavior.
The difference in electrical conductivity between metal and liquid slag is about four orders of magnitude. Therefore, the method chosen to calculate an average cell electrical conductivity will have a great impact on the computed electromagnetic field. For instance, using an arithmetic average, a cell located in the slag phase and containing 0.1 vol% liquid metal would be assigned a value of around $10^3\ \Omega^{-1}.m^{-1}$, while the harmonic average would lead to roughly the same value as the liquid slag ($250\ \Omega^{-1}.m^{-1}$).

At the electrode tip, a liquid film is formed. In such cells, one can consider that the electric current successively crosses the liquid metal film and the slag. In that case, the electrical circuit is formed by two consecutive resistances (one representing the metal film, the other one the slag phase). The equivalent cell electrical conductivity is therefore a harmonic average of each phase conductivity. Underneath, when drops are forming, liquid metal forms so-called faucets. In such cells, this phenomenon is better modeled considering two parallel electrical resistances (one for the liquid metal column and the other for the surrounding slag). Arithmetic average is then used to estimate the cell electrical conductivity.
For isolated droplets (i.e. everywhere else in the slag domain), the equation 4 proposed by Maxwell [14] is used. It has been derived considering the behavior of a conducting spherical particle in a dielectric medium.

$$\sigma_{cell} = \frac{\sigma_{slag}\left(\frac{2}{\sigma_{metal}} + \frac{1}{\sigma_{slag}} - 2\alpha_{metal}\left(\frac{1}{\sigma_{metal}} - \frac{1}{\sigma_{slag}}\right)\right)}{\frac{2}{\sigma_{metal}} + \frac{1}{\sigma_{slag}} + \alpha_{metal}\left(\frac{1}{\sigma_{metal}} - \frac{1}{\sigma_{slag}}\right)} \quad (4)$$

In the equation above, α represents the volume fraction of the phase indicated in subscript.

The corresponding current densities are then calculated for each phase, to compute distinct Lorentz forces and Joule effect. In the case of metal droplets, the computed electromagnetic forces are multiplied by $^3/_2$ to take into account the pressure gradient created in this enclosed conductive fluid [15]. The expected highest Lorentz forces are those created by the current going through liquid metals faucets.

Liquid Film Dynamics

Liquid film and droplets hydrodynamics are undoubtedly different in nature, hence their interactions with the continuous phase. As the aim is to represent the liquid film within the Euler-Euler model, momentum equations will suffer some modifications.

Classically, the behavior of a liquid film can be described by the Saint-Venant equations system, when the film height is smaller than the propagation length scale [16]. It consists of a continuity equation (representing the transfer of the film height) and a momentum equation, often named "shallow water equations". The latter is derived from the integration of the Navier-Stokes equations along the liquid film height.

The continuity equation of this shallow water system, written for a 1D case in cylindrical coordinates, reduces to Equation 5.

$$\frac{\partial h_{film}}{\partial t} + \frac{1}{\mathrm{r}}\frac{\partial}{\partial r}\left(r u_r h_{film}\right) = 0 \quad (5)$$

In order to reduce the momentum conservation equation of the dispersed phase to the shallow water one, the drag force is set to zero and an interfacial viscous momentum exchange is added. Furthermore, axial velocity must become negligible.

Interfacial tension between slag and metal is very high. Even though its density is higher than the slag one, the liquid metal film remains stable as long as the interfacial tension compensates its weight. The axial velocity of the liquid film can therefore be neglected when the height of the latter is lower than a critical one.

Explicitly modeling interfacial tension is very challenging in a 2D Eulerian model, as the curvature of the liquid metal film is not simulated. Therefore, only its effect is accounted for, as a force acting against gravity and compensating the density difference between phases when the film height is lower than its critical value, which can be estimated from the 3D simulations.

3D to 2D: Comparison

3D VOF simulation as well as the enhanced 2D Euler-Euler model have been used to calculate the liquid metal and slag flows for the same industrial configuration. The electrode diameter is 430 mm and the mold inner diameter is 530 mm. Input processing parameters are determined thanks to a trial remelting operation, processed at Aubert & Duval facility, presented in the experimental section of this article.

Both models predict, for these operating parameters, a concentration of liquid metal droplets in a restricted area of the ingot, as illustrated by Figure 3. Moreover, thanks to the accurate description of the liquid film hydrodynamics described above, in both cases the gathering of liquid metal film toward the center is the predominant effect. Lorentz forces acting on liquid metal faucets are also of importance.

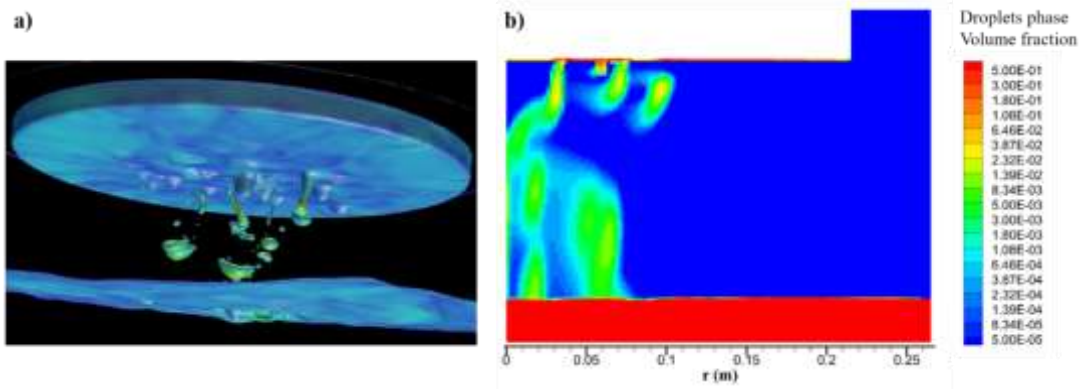

Fig. 3: Comparison of liquid metal droplets repartition obtained by a) by 3D simulations and b) the enhanced 2D model

A quantitative comparison of the results given by 3D simulations and 2D modeling is not presented here, as it may not be very accurate. For example, droplets velocities computed by the 2D model are dependent on the chosen diameter, while in 3D simulation droplet morphology is computed, and the "dispersed phase" is constituted by a large distribution of size. Nonetheless, we can underline than the predicted velocities are within the same order of magnitude (10^{-1} m.s^{-1}).

Example of Applications

Since the 2D diphasic model provides a good level of information and is much less computationally expensive than DNS 3D simulations, we have used it to estimate the influence of various parameters on the droplets behavior. In the following, variations in the droplet size and the electrode immersion are investigated.

Influence of Droplet Size

It is well known that, during remelting, droplets are formed within a wide size range: typical diameter ranges from 1 to 10 mm [17]. As this diameter has a strong influence on the momentum exchange, it is expected to have also a strong impact on the predicted overall behavior.

As we can see in Figures 4 a) and b), considering respectively 1 mm and 5 mm diameter droplets, the computed distribution of the time-averaged volume fraction of liquid metal within the slag is different. Small droplets are more easily carried by the slag flow, whereas bigger ones fall almost vertically through the slag bath. Nonetheless, large droplets have a strong impact on slag hydrodynamics. Therefore, considering only small metal droplets might not give a fully accurate distribution, as they can be entrapped within the trail of bigger ones.

Impact of Electrode Immersion Depth

The 2D Euler-Euler model has also been applied to simulate two different electrode immersion depth (15 mm and 50 mm). The distributions of droplets through the slag are illustrated by the volume fraction fields in Figures 4 b) and c).

In both cases, the liquid film is gathered toward the center and droplets fall from a restricted area. This “dripping area” seems to be slightly affected by the electrode immersion depth.

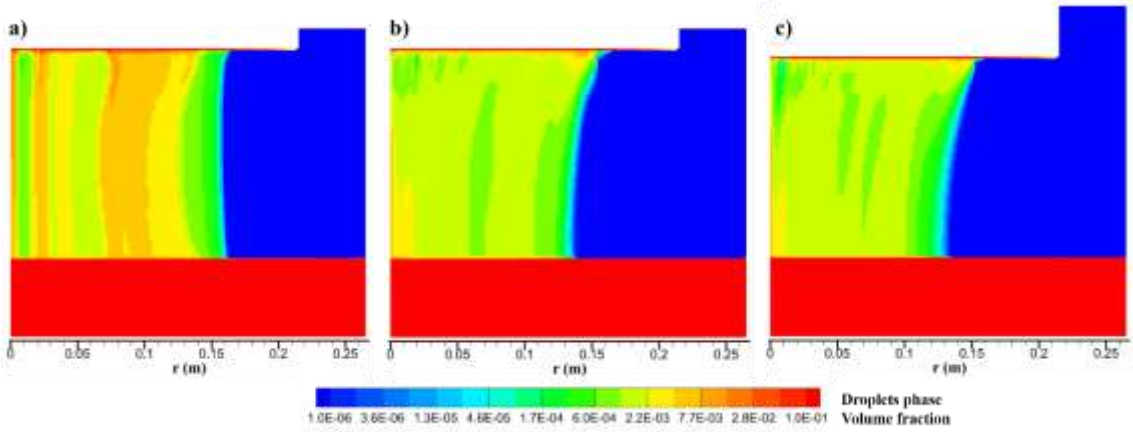

Fig. 4: Time-averaged liquid-metal volume fraction fields for a) 15 mm immersion and 1 mm droplets, b) 15 mm immersion and 5 mm droplets and c) 50 mm immersion and 5 mm droplets

Experimental Work

To support the development of the previously described models, several trial ingots have been recently remelted at Aubert & Duval facility. This experimental campaign focuses on the impact of electrode immersion depth and fill ratio on remelting procedure and ESR ingots quality. These trials were not only designed to better understand the remelting process and its control, but also to gather experimental data within a wide range of operating conditions. They are used as input and comparison data for the development of the new diphasic models, as it is supposed that such variations of immersion depth or fill ratio may affect droplets behavior. These trial remeltings will then help validate the final engineering model.
In this paper, we will only consider the investigations on the influence of the electrode immersion depth on electrical signals and ingot surface aspect. A more comprehensive study will be the topic of a future publication.

During remelting, immersion cannot be directly measured. In order to keep it constant, we chose to control the ram movement through the voltage signal. Industrial remeltings are often controlled through the voltage swing, but for these trials, a less-processed signal was preferred. A steady voltage during a certain duration means a constant immersion depth (if both the electric current and slag resistivity remain constant). More precisely, this steady voltage reflects a stable gap between the electrode tip and the ingot.
During these trials, melt rate was not controlled, hence it resulted from a constant electric current.

In the first trial, the fixed current stage was divided into three segments, each one with a distinct immersion. The evolution of voltage, current and the resulting melt rate (smoothed curves) are plotted in Figure 5 a). The melt rate measured by the load cell system was disrupted by the variations in electrode immersion depth, as they generated variations in Archimedean buoyant force. At the end of each constant immersion segment, the pool profile was marked by adding Ni pellets.

Ingot expertise showed that the melt pool seemed mostly affected by the variation of melt rate induced by these three different immersion depths. No significant variation in the melt pool shape was found.

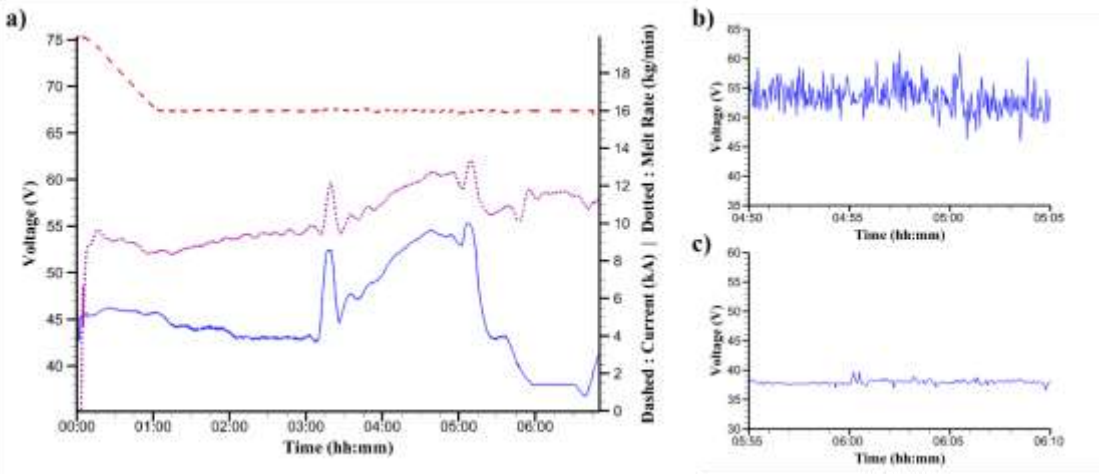

Fig. 5: a) Evolution of voltage, electric current and melt rate for the first remelting (smoothed curves) and details of voltage for b) a shallow immersion and c) a deeper immersion

A second trial was based on slow continuous variations of immersion, by setting voltage slopes. As the voltage is increased, electrode immersion depth is lowered (and vice-versa).
At shallow immersion, voltage is high and an important swing is observed. The slag surface movements create a variation in the immersed area, which causes the natural swing. Air entrapment under the electrode, as it increases the electrical resistance, is also a source of swing. An example of the temporal evolution of voltage, recorded while the immersion was shallow, is shown in Figure 5 b).
On the opposite, when the immersion is deeper, electrical signals are flat. The slag surface motion is of less importance, and air entrapment is unlikely to occur. An example of the temporal evolution of voltage when at such an immersion depth is shown in Figure 5 c).

A good ingot surface can be achieved if the slag skin is partially remelted [1, 18, 19]. The ingot surface is an important quality criterion. The immersion depth greatly affects heat distribution in the slag.

- When the immersion is shallow, a good surface quality is usually obtained and the slag skin is thin.
- When it is deeper, the solidified slag is thicker, and liquid metal head is not likely to exist. Wrinkles surrounding the entire ingot can be observed.

In both configurations, details of ingot surface aspect are shown in Figure 6.

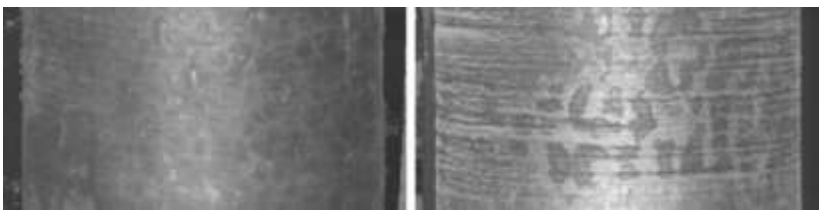

Fig. 6: Example of ingot surface aspect using a) a shallow and b) a deeper immersion

Conclusion and Prospects

In this paper, the development of a new model was addressed, based on the comparison with results obtained thanks to 3D detailed simulations of the dripping phenomena in ESR. This model, based on an Euler-Euler approach with accurate adaptations to represent the liquid film dynamics, is a preliminary stage before a full integration in the engineering model SOLECS, easy to use by the industrial partners. The final goal of this study is to model the impact of a non-homogeneous distribution of droplets on the ingot metallurgical quality, and to finally predict the behavior of droplets with changing operating conditions.
In the near future, this diphasic model will be simplified into a mixture model, in order to be more easily implemented into SOLECS. Eventually, one will be able to study the impact of the droplet distribution evolution with the operating parameters on the final ingot quality.

This improved engineering model will be supported by new trial ingots, with a large variation in the operating parameters in order to quantify their impact on ingot quality (the melt pool profile, among others).

References

1. G. Hoyle, *Electroslag Processes: principles and practice* (London: Applied Science Publishers, 1983).
2. A.S. Ballantyne, Ph.D. thesis (University of British Columbia, 1978).
3. A. Jardy, Ph.D. thesis (Institut National Polytechnique de Lorraine, 1984).
4. V. Weber, Ph.D. thesis (Institut National Polytechnique de Lorraine, 2008).
5. A.H. Dilawari, J. Szekely, *Met. Trans. B*, 9 (1) (1978), 77-87.
6. A. Kharicha et al., *Proc. Int. Symp. Liquid Metal Processing and Casting*, Nancy, France (2007), 113-119.
7. E. Karimi Sibaki et al., *Proc. Int. Symp. Liquid Metal Processing and Casting*, Austin, Texas (2013), 13-19.
8. N. Giesselmann et al., *ISIJ International*, 55 (7) (2015), 1408-1415.
9. A. Kharicha, A. Ludwig, M. Wu, *Proc. Int. Symp. Liquid Metal Processing and Casting* Nancy, France (2011), 41-48.
10. V. Weber et al., *Met. and Mat. Trans. B*, 40 (3) (2009), 271-280.
11. M. Hugo et al., *Met. and Mat. Trans. B*, 47 (4) (2016), 2607-2622.
12. L. Schiller, A. Naumann, *Z. Ver. Deutsch. Ing.*, (77) (1933), 318-320.
13. W.E. Ranz, W.R. Marshall, *Che. Eng. Prog.*, 48 (3) (1952), 141-146.
14. J.C. Maxwell, *A treatise on electricity and magnetism* (London: Clarendon Press, 1873).
15. A. Kolin, *Science*, 117 (3032) (1953), 134-137.
16. H. Chanson, *Hydraulics of Open Channel Flow* (London: Butterworth-Heinemann, 2004).
17. A. Kharicha et al., *Proc. Int. Symp. Liquid Metal Processing and Casting*, Santa Fe, New Mexico (2009), 235-242.
18. J. Cameron, M. Etienne, A. Mitchell, *Met. Trans*, 1 (7) (1970), 1839-1844.
19. A. Kharicha et al., *Int. Conf. Ingot Casting Rolling Forging*, Milan, Italy (2014).